Real-space measurement of the potential distribution inside organic semiconductors

Real-Space Measurement of the Potential Distribution Inside Organic Semiconductors

M. Kemerink,[1] P. Offermans,[1] J. K. J. van Duren,[2] P. M. Koenraad,[1] R. A. J. Janssen,[2]
H. W. M. Salemink,[1] and J. H. Wolter[1]

[1]*COBRA Inter-University Research Institute, Department of Physics, Eindhoven University of Technology, P.O. Box 513, NL-5600 MB Eindhoven, The Netherlands*

[2]*Laboratory of Macromolecular and Organic Chemistry, Eindhoven University of Technology, P.O. Box 513, NL-5600 MB Eindhoven, The Netherlands*

(Received 7 September 2001; published 14 February 2002)

We demonstrate that the soft nature of organic semiconductors can be exploited to directly measure the potential distribution inside such an organic layer by scanning-tunneling microscope (STM) based spectroscopy. Keeping the STM feedback system active while reducing the tip-sample bias forces the tip to penetrate the organic layer. From an analysis of the injection and bulk transport processes it follows that the tip height versus bias trace obtained in this way directly reflects the potential distribution in the organic layer.

DOI: 10.1103/PhysRevLett.88.096803 PACS numbers: 73.61.Ph, 68.37.Ef, 71.20.Rv

One can identify two approaches to the investigation of charge transport in organic semiconductors. On the one hand, there is a large body of work on bulk devices, in the simplest case consisting of an organic layer, with a typical thickness d of 100 nm, sandwiched between two metallic electrodes [1,2]. Obviously, the spatial resolution is extremely limited in such experiments [3,4]. On the other hand, highly local techniques like scanning-tunneling microscopy (STM) are often used for the investigation of the electronic structure of individual molecules [5]. In this case, samples with a single (sub-)monolayer of organic molecules on a conductive substrate are used. It was shown in the pioneering work of Alvarado *et al.* that STM on layers of "device" thickness can be a bridge between these two approaches [6,7]. By ramping the tip-sample bias with the STM feedback system enabled, a so-called tip height vs bias (z-U) curve is obtained. The authors identified the plateaus in z-U curves as the single particle band gap and found strong microscopic fluctuations in this gap, related to spatial inhomogeneities [7].

In this Letter we report on combined spectroscopic measurements by STM on 2-methoxy 5-(3',7'dimethyloctyloxy)-1,4-phenylene vinylene (MDMO-PPV) on gold substrates and perform, for the first time, a detailed analysis of the functional shape of tip height-bias curves. We find that these curves directly reflect the normal component of the potential distribution in the polymer at the start of the z-U measurement. Moreover, we have developed a theoretical model that consistently describes these experiments. Our results are valid independent of the particular tip, substrate, and organic materials used.

Our samples consist of a glass substrate, on which a 100 nm gold electrode is evaporated at 10^{-6} mbar. On top of the metal electrode a MDMO-PPV layer is spin coated from hot (60 °C) orthoxylene under ambient conditions. All STM experiments are performed at room temperature in the dark, in helium gas. However, the samples are transported and mounted under ambient conditions, leading to a total exposure time to air of about 15 min. The tunneling tips, which act as counterelectrode, are etched from 0.15 mm Pt wire. The tip is virtually grounded and the bias U is applied to the substrate. From scanning-electron microscopy measurements we found that our tips are very smooth and typically have an apex radius of 50 nm. All spectroscopic curves are taken during scanning a 25×25 nm area and averaged over multiple curves taken on a 8×8 or 16×16 grid, unless stated otherwise. In intrinsically disordered materials like the films used here, no effects of increased disorder due to the penetration of the tip are observed. This is in contrast with similar measurements performed on poly(3-hexylthiophene) where the intrinsic ordering [8] is clearly destroyed after the first penetration of the tip.

The model we use to interpret our data takes both the current injection process at the metal-polymer interface and the conduction in the bulk of the polymer explicitly into account; see the inset of Fig. 1. Since both Pt and Au are high work function metals the electron injection can be neglected and only the hole current is considered. The injection current equals the sum of the tunneling, thermionic, and interface recombination currents and is basically calculated as indicated in Ref. [9]. However, the tunneling component is calculated in the WKB approximation, as described in Ref. [10]. For the present problem this extension is essential, since it allows us to deal with arbitrary injection barriers. The effect of the barrier lowering by the image force on the injection current has been taken into account. The bulk current is described in terms of space-charge limited conduction (SCLC) with a mobility that depends on the local electric field as $\mu(E) = \mu_0 \exp(\gamma E^{1/2})$ [1]. The injection and bulk regions are matched by the demands of current, field, and potential continuity. Our model can be regarded as an extension of the work of Datta *et al.* [5] to layers consisting of many molecules. In Ref. [5] it is shown that the electrostatic potential of a single dithiol molecular layer on a gold

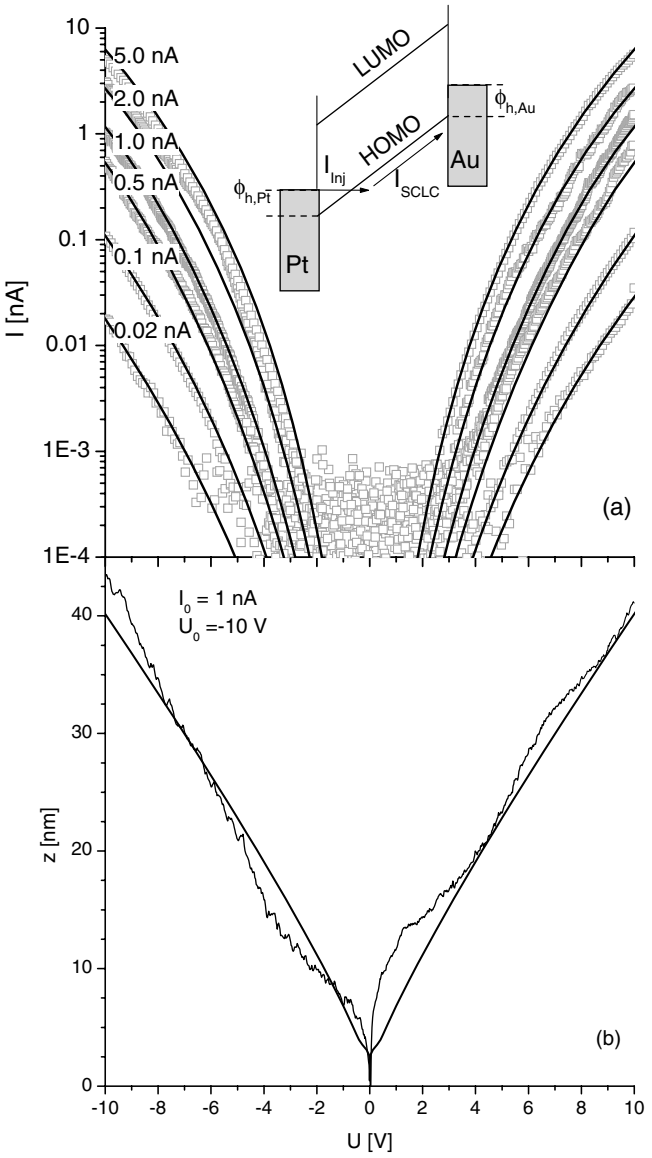

FIG. 1. (a) I-U characteristics. The current set point at $U = 10$ V is indicated on the left-hand side. The symbols are experimental data; the solid line is the result of the numerical model. The inset schematically shows the band diagram under forward bias. (b) z-U measurement on the same sample. For both calculations: $\phi_{h,\mathrm{Pt}} = \phi_{h,\mathrm{Au}} = 0.5$ eV.

substrate is not equal to that of the metallic substrate, but in between that of the substrate and the tip. It will, however, become clear that a model that simply determines the electrostatic potential in the polymer layer by linear interpolation between substrate and tip [5,11] cannot describe our experimental findings.

Figure 1 shows a typical result of combined I-U and z-U measurements. The thick solid lines are the results of our model calculations using $\mu_0 = 5 \times 10^{-11}$ m^2/V s and $\gamma = 5.4 \times 10^{-4}$ (m/V)$^{1/2}$, which are taken from Ref. [12]. The density of states (DOS) in the bulk is taken $N_{\mathrm{DOS}} = 1 \times 10^{27}$ m^{-3} [9]. The barrier heights for injection from substrate, $\phi_{h,\mathrm{Au}}$, and tip, $\phi_{h,\mathrm{Pt}}$, and the tip-sample separation are used as adjustable parameters [13]. The values found for $\phi_{h,\mathrm{Au}}$ and $\phi_{h,\mathrm{Pt}}$ agree well with values obtained from device modeling [1] and internal photoemission [2]. Moreover, the low injection barriers found justify the assumption of unipolarity. It is apparent that the description of the I-U characteristics by the model is excellent over 4 orders of magnitude. The calculated z-U curve, however, lacks the structure that is present in the experimental curve, although the average slope of both branches is reproduced. Thus, it is essential to discuss which information can be extracted from z-U curves.

Below, it is demonstrated that z-U curves directly reflect the normal component of the potential distribution that is present between tip and sample electrode at the starting point of the z-U measurement. The injection barrier, and thus the injected current, depends only on the local field E_0 at the injecting contact and material properties, of which the barrier height for injection is the most important. Since the feedback loop is enabled during a z-U measurement, the (injected) current has to remain constant, and thus E_0 has to stay constant at all U. In other words, the injection barrier is always the same for a given current. For SCLC transport in homogeneous materials the potential is fully determined by the current density, the field E_0 at the injecting contact, and, again, material properties. Since these are all constants during the measurement, the potential that extends down into the polymer from the injecting contact is fixed, up to the counterelectrode. This is illustrated in Fig. 2. The alignment of the highest occupied molecular orbital (HOMO) and lowest unoccupied molecular orbital (LUMO) levels with the counterelectrode is also a given quantity ($\phi_{h,s}$ and $\phi_{h,t}$, respectively, in Fig. 2). Therefore, the only possibility to keep the current constant with changing bias is to move the tip backward or forward, exactly following the potential distribution, as shown by traces A and B in Fig. 2. Summarizing, the tip movement with changing bias is directly linked to the fixed potential distribution, which extends from the injecting electrode down into the polymer.

Now that z-U curves are shown to directly reflect the potential distribution between tip and sample, the wiggles in the experimental z-U curves are, via Poisson's law, directly related to the presence of additional charges in the sample. We have extended our model to account for the additional band bending due to these charges. We assume that the charges are distributed in half-Gaussian profiles at each of the injecting contacts. The charges at the tip side follow the tip movement. From fitting to the data a peak density of $0.06 N_{\mathrm{DOS}}$ and a width of 4 nm are found. The negative and positive charges are present at the positive (injecting) and the negative (collecting) electrode, respectively. With this extension, the experimental curves are reproduced very well, as is shown in Fig. 3. The asymmetry around zero bias is reproduced by the choice of a smaller barrier for gold than for platinum. The nature of the additional charges is uncertain at present; possibly they arise from charge trapping on oxygen-related defects

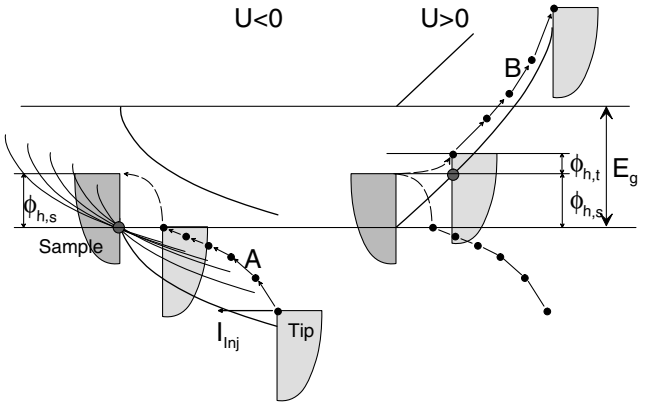

FIG. 2. Schematic band diagram, showing the direct link between the potential in the polymer and measured z-U curves. The upper (lower) thick curve is the LUMO (HOMO) level; the light (dark) gray area is the tip (sample) density of states, up to the Fermi level.

that are present in our samples due to the exposure to air. Alternatively, the positive charges could be explained by band bending due to the proximity of the metal electrode [14]. A possible mechanism to stabilize charge near the metal-polymer interface is the formation of a bipolaron lattice [15,16]. Interestingly, both the length scale and the amount of charge that we find from our modeling agree extremely well with those reported for such a bipolaron lattice [14,15]. Finally, we stress that the curves in Fig. 1(a) are calculated without additional charges. Although they are apparent in the z-U curves, these charges do not have a clear signature in the I-U curves. This is particularly important since I-U spectroscopy is the most common measurement on devicelike structures.

We now discuss the spreading in the individual I-U and z-U curves. In Fig. 4 the individual I-U curves contributing to the average curve in Fig. 1(a) are shown. Although the curves cross the set point I_0 at $+10$ V, there is a large spread at lower biases. These fluctuations appear to be totally random, and no spatial dependence was observed: taking consecutive I-U curves at one position yielded similar results. Therefore, we interpret these as the effect of random fluctuations in the molecular conformation at the injecting contact. Combining the experimental data and the model calculations we deduct barrier height variations of ± 0.05 eV. Since the current has to be 1.0 nA at 10 V, this translates to a variation in the tip-substrate distance of 2 nm. The variation obtained in this way agrees very well with the observed spreading of 3 nm in the individual z-U curves; see Fig. 3. Here, the fluctuations are not only driven thermally, but also by the downward movement of the tip. Since their magnitude is very similar to that obtained from the analysis of the I-U curves, it is reasonable to assume that they have the same origin. Most likely, different arrangements of the molecules close to the injecting contact show up as variations in the injection barrier height. In large area devices these fluctuations will be averaged out.

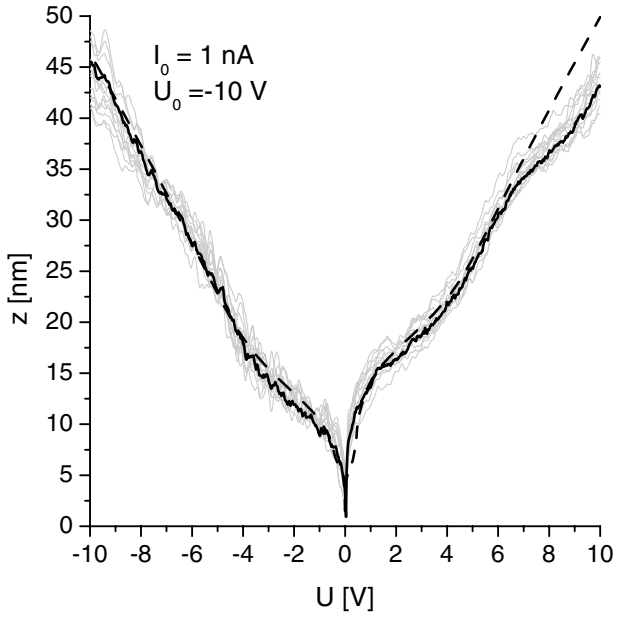

FIG. 3. Same data as in Fig. 1(b). The thin gray lines are individual measurements; the thick solid line is their average. Calculation (dashed line) with additional charges near both electrodes; see text. $\phi_{h,\mathrm{Pt}} = 0.5$ eV, $\phi_{h,\mathrm{Au}} = 0.15$ eV; other parameters as in Fig. 1.

It is known that, depending on the injection barrier height, either the injection or the bulk transport can be the current limiting process in organic material-based devices [1]. In Fig. 5 calculated z-U curves are plotted for tip injection barriers from 0.25 to 1.5 eV.

For hole injection, and coming from large biases, a plateau sets in as soon as the Fermi level of the *injecting* contact aligns with the HOMO level at the collecting

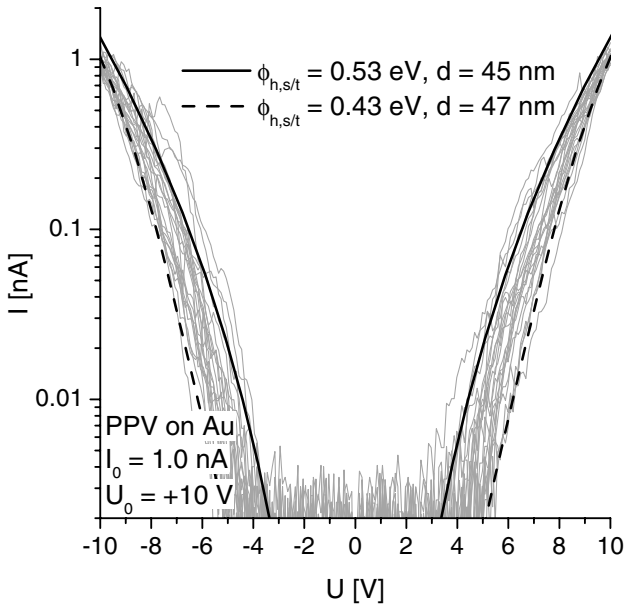

FIG. 4. Individual I-V curves. The thick lines are calculations with different injection barriers and sample thickness. Unspecified parameters as in Fig. 1.

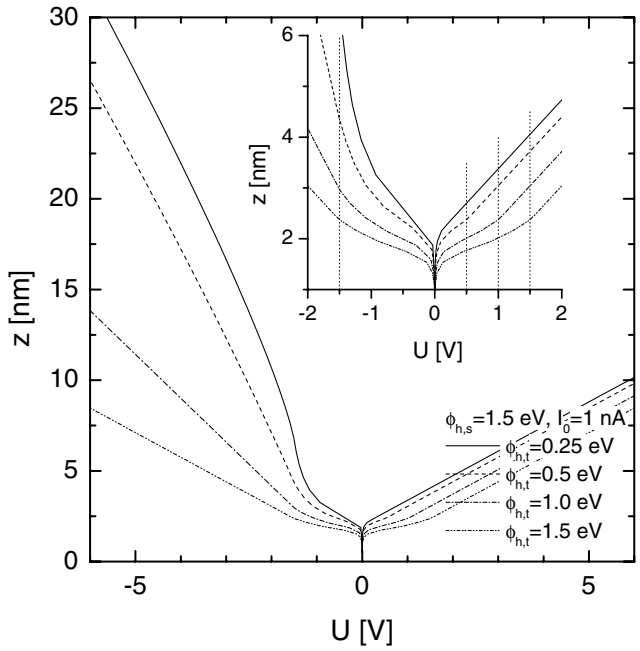

FIG. 5. Calculated z-U curves, without additional charges. The inset is a zoom-in at low bias. Unspecified parameters as in Fig. 1.

contact, i.e., as soon as direct tunneling to the collecting contact is possible; see also Fig. 2. The width of the plateau in Fig. 5 thus reflects the alignment of the HOMO level with the Fermi level of the *collecting* contact, which is simply the hole injection barrier of that contact [17]. For unipolar devices, as discussed here, the plateaus at positive and negative bias add up to the sum of the injection barriers of the dominant carrier. When the tip dominates the injection process at both polarities [18], the sum equals the single particle band gap [7]. Calculations beyond the planar model used here [19] show that when $z \lesssim R_{\mathrm{tip}}$ injection is dominated by the contact with the lowest injection barrier, and that the planar model is sufficient. On the other hand, when $z \gg R_{\mathrm{tip}}$ field enhancement at the tip apex can lead to a dominance of injection from the tip at both polarities.

The curvature of the bands that is characteristic for SCLC is reflected in the curved z-U spectra obtained at negative bias for low $\phi_{h,t}$, i.e., 0.25 and 0.5 eV. For higher injection barriers the current is no longer space-charge limited, but injection limited, and the bands and thus the z-U curves become straight. In this case, the slope is the reciprocal of the field E_0 that is needed to inject the required current. Thus, with increasing barrier height, the slope at *negative* polarity decreases. Note that the height of the barrier shows up in the plateau width at *positive* polarity, which develops with increasing $\phi_{h,t}$; see the inset of Fig. 5.

Summarizing, combined spectroscopic measurements are performed on MDMO-PPV layers on Au substrates. We find that z-U curves directly reflect the potential distribution between tip and sample electrode. This provides one the unique possibility to directly measure $V(z)$ inside a polymer device under operational conditions. Moreover, the spreading in both I-U and z-U curves as discussed is explained in terms of fluctuations in the molecular arrangement at the injecting contact. Finally, the transition from space-charge limited to injection limited conduction is discussed.

The research of Dr. M. Kemerink has been made possible by the Royal Netherlands Academy of Arts and Sciences.

[1] P. W. M. Blom and M. C. J. M. Vissenberg, Mater. Sci. Eng. **27**, 53 (2000).
[2] I. H. Campbell and D. L. Smith, Solid State Phys. **55**, 1 (2001).
[3] F. Feller, D. Geschke, and A. P. Monkman, Appl. Phys. Lett. **79**, 779 (2001).
[4] M. Hiramoto, K. Koyama, K. Nakayama, and M. Yokoyama, Appl. Phys. Lett. **76**, 1336 (2000).
[5] S. Datta, W. Tian, S. Hong, R. Reifenberger, J. I. Henderson, and C. P. Kubiak, Phys. Rev. Lett. **79**, 2530 (1997).
[6] S. F. Alvarado, P. F. Seidler, D. G. Lidzey, and D. D. C. Bradley, Phys. Rev. Lett. **81**, 1082 (1998).
[7] S. F. Alvarado, S. Barth, H. Bässler, U. Scherf, J.-W. van der Horst, P. A. Bobbert, and M. A. J. Michels, Adv. Func. Mat. **12**, 117 (2002).
[8] H. Sirringhaus *et al.,* Nature (London) **401**, 685 (1999).
[9] P. S. Davids, I. H. Campbell, and D. L. Smith, J. Appl. Phys. **82**, 6319 (1997).
[10] R. M. Feenstra and J. A. Stroscio, J. Vac. Sci. Technol. B **5**, 923 (1987).
[11] R. Rinaldi, R. Cingolani, K. M. Jones, A. A. Baski, H. Morkoc, A. Di Carlo, J. Widany, F. Della Sala, and P. Lugli, Phys. Rev. B **63**, 075311 (2001).
[12] P. W. M. Blom, M. J. M. de Jong, and M. G. van Munster, Phys. Rev. B **55**, 656 (1997).
[13] The actual barrier height depends, via the image force, on the field at the injecting contact. With ϕ_h the difference between the HOMO level and the metal Fermi level is meant.
[14] Y. Park, V. Choong, E. Ettedgui, Y. Gao, B. R. Hsieh, T. Wehrmeister, and K. Müllen, Appl. Phys. Lett. **69**, 1080 (1996).
[15] M. N. Bussac, D. Michoud, and L. Zuppiroli, Phys. Rev. Lett. **81**, 1678 (1998).
[16] P. S. Davids, A. Saxena, and D. L. Smith, Phys. Rev. B **53**, 4823 (1996).
[17] One would expect plateaus of width 0.1–0.5 eV at both sides of $U = 0$. From Figs. 1(b) and 3 it is clear that the resulting plateaus are beyond experimental resolution. With the low-work-function metal Yb for electrode material, a plateau of about 3 eV was observed at negative bias, as expected (not shown).
[18] S. F. Alvarado, L. Rossi, P. Müller, P. F. Seidler, and W. Riess, IBM J. Res. Dev. **45**, 89 (2001).
[19] M. Kemerink *et al.* (unpublished).